Electronic supplement to "Tropical troposphere to stratosphere transport of carbon monoxide and long-lived trace species in the Chemical Lagrangian Model of the Stratosphere (CLaMS)"

by Pommrich et al.

The purpose of this electronic supplement is twofold; first a climatology of radical species is presented. This climatology is required for the formulation of the simplified chemistry presented in the main body of the paper. Second, a number of additional figures is presented, complementing the information in the main body of the paper.

1 Description of the climatology of radical species

The radical species climatology in this supplement provides monthly averages of the radical species OH, HO_2, O(1D), Cl, and the air molecule total number density (TND). The averages are calculated from hourly output from a chemistry simulation of the Chemical Lagrangian Model of the Stratosphere (CLaMS) (McKenna et al., 2002), thus also averaged over the diurnal cycles. They can be used to calculate simplified chemistry e.g. first order loss reactions of longlived chemical tracers. The simulation was initialised with the species O_3, CH_4, H_2O, HCl, NOx from the HALOE climatology (Grooß and Russell, 2005). The remaining chemical species were initialised from the Mainz 2-D photochemical model (Grooß, 1996). The chemistry integration was performed using the SVODE solver scheme (Brown et al., 1989) and no advection of the air parcels was considered. The HALOE ozone climatology (Grooß and Russell, 2005) was also used in the radiative transfer calculation to determine the photolysis rates.

The file (radical_species_climatology.nc) contains 18 latitude bins from 85°S to 85°N, 34 pressure bins from 980 hPa to 0.18 hpa for each of the 12 months. The file format is NetCDF.

2 Additional figures

2.1 Comparison of CLaMS results with COLD CO measurements

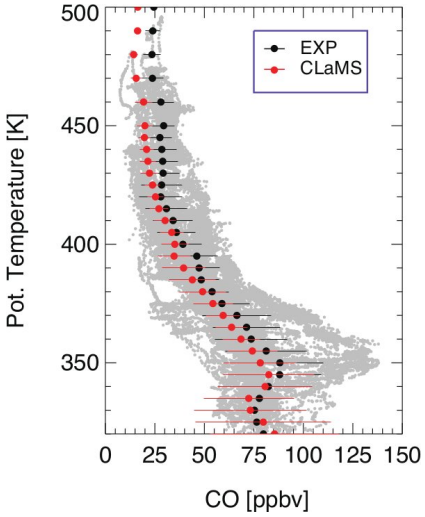

Figure 1: Climatological comparison of vertical CO profiles measured by the COLD instrument aboard the Geophysica aircraft in the tropical tropopause region with CLaMS simulations. The climatology of CO measurements (grey dots) is based on the COLD measurements in the campaigns TROCCINOX (February 2005, Konopka et al., 2007), SCOUT-O3 (November 2005, Brunner et al., 2009) and AMMA (Summer 2006, Cairo et al., 2010). The vertical profile of the mean of all CO measurements is shown as black symbols with the horizontal bars denoting the standard deviation of the mean. The corresponding model values (derived by interpolating the model information on the location and time of the measurements) are shown in red.

In the main body of the paper, the CLaMS model results for CO are compared with in situ measurements flight by flight for the TROCCINOX campaign (Fig. 4 in the main body of the paper) and as a campaign climatology for SCOUT-O3 and AMMA (Fig. 5 in the main body of the paper). For completeness, we show below the climatological comparison for all campaigns (Fig. 1) and the comparison on a flight by flight basis for SCOUT-O3 and AMMA (Figs. 2 to 4).

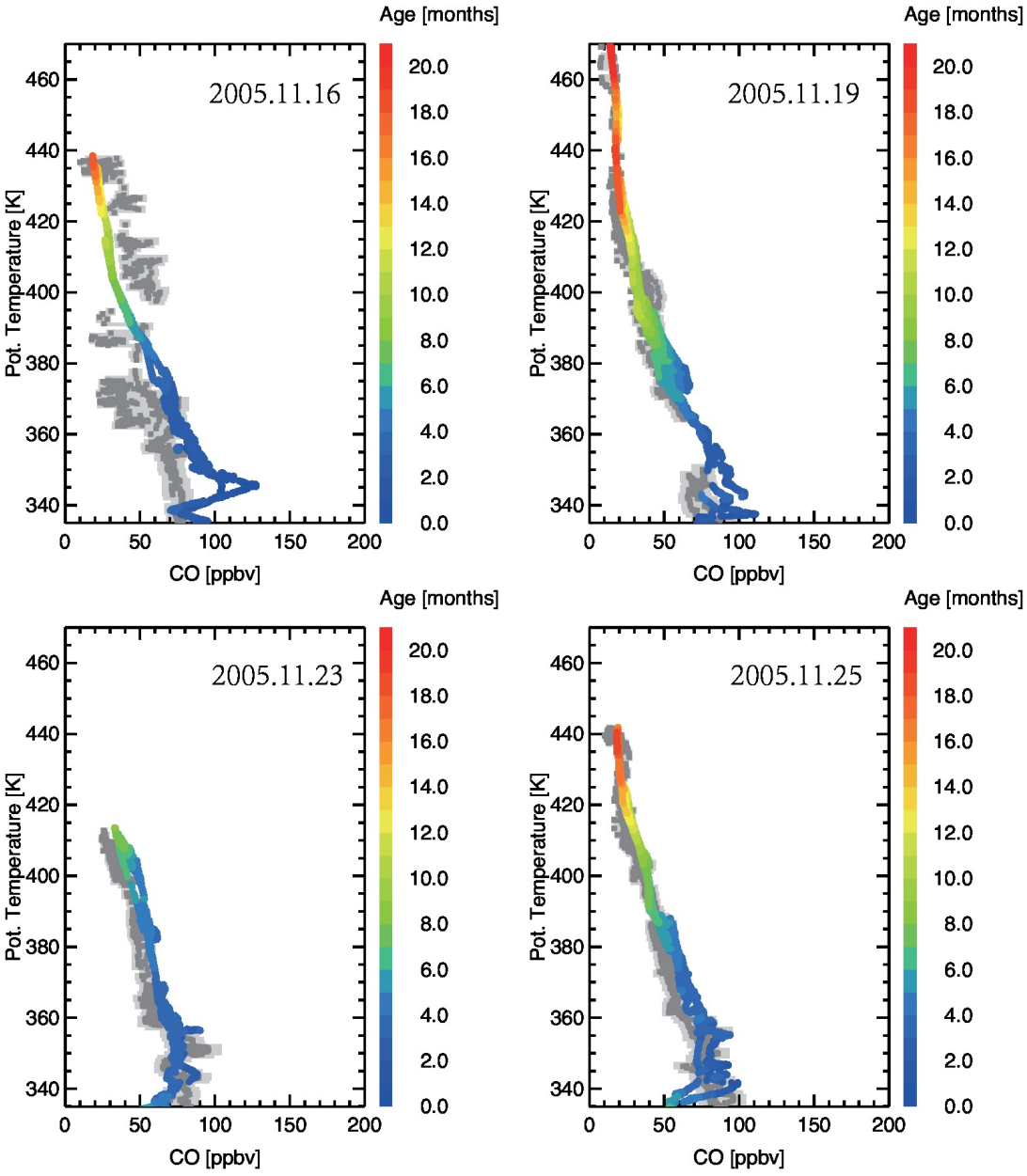

Figure 2: Comparison of the simulation of CO from CLaMS (coloured) with in-situ measurements from the COLD instrument (dark grey) for the first four flights during the SCOUT-O3 campaign. The mean age of air calculated by the model is colour-coded and given in months. The absolute in-flight accuracy for the COLD CO measurements is about 9% and is indicated as a light grey shading.

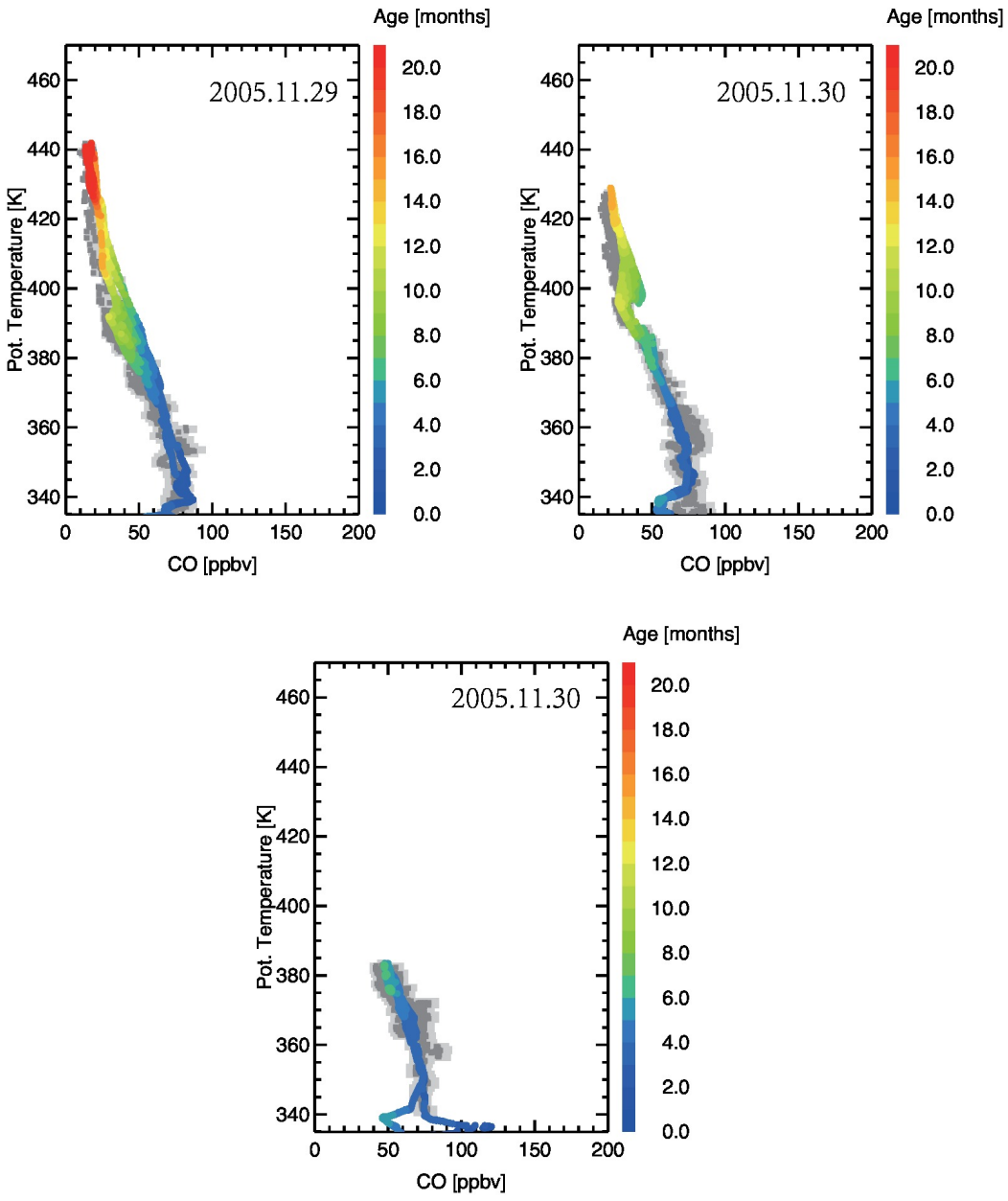

Figure 3: As Figure 2, but for the last three flights during the SCOUT-O3 campaign.

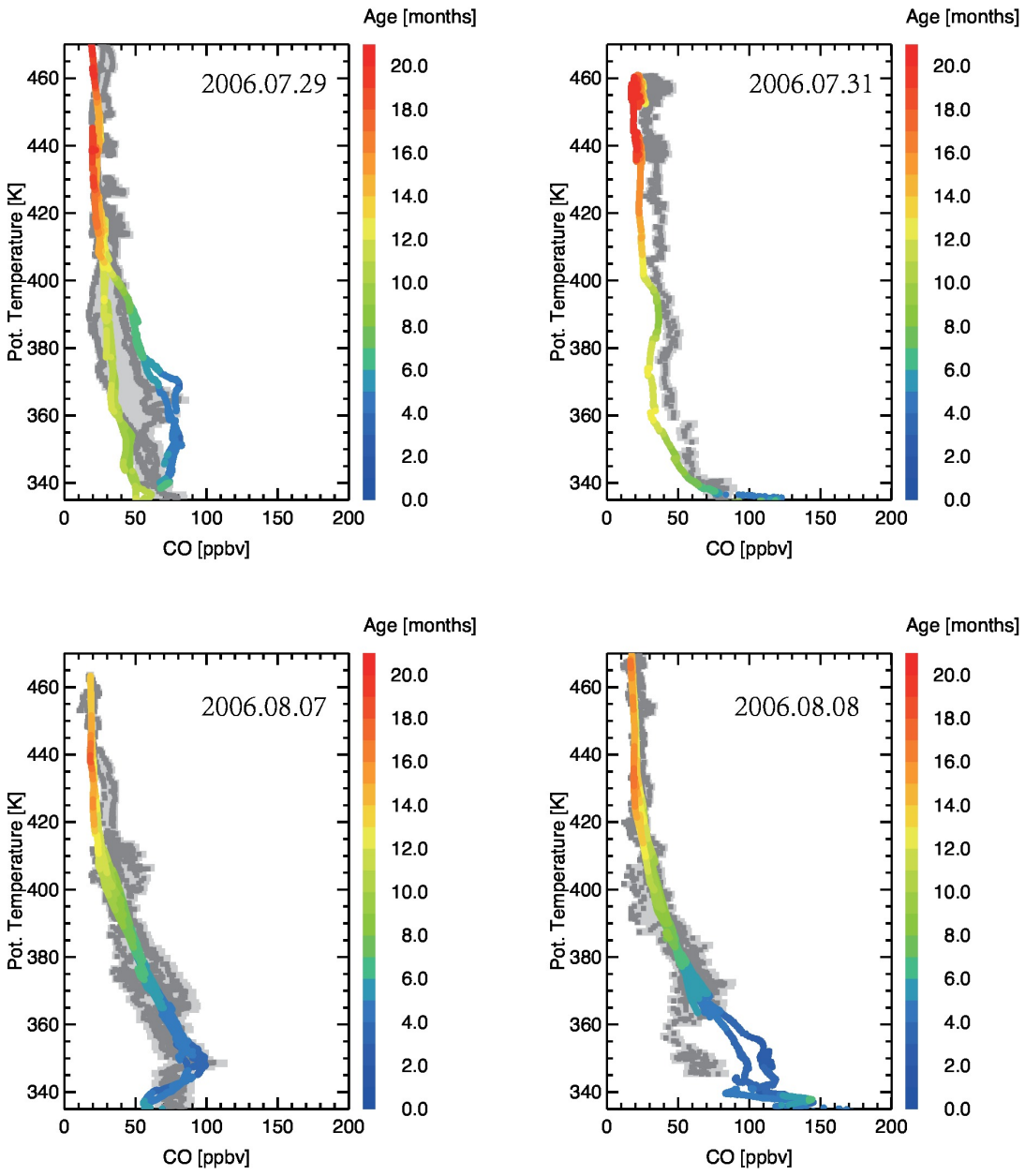

Figure 4: As Figure 2, but for the AMMA campaign.

2.2 Tape recorder patterns for different Lagrangian grid formulations

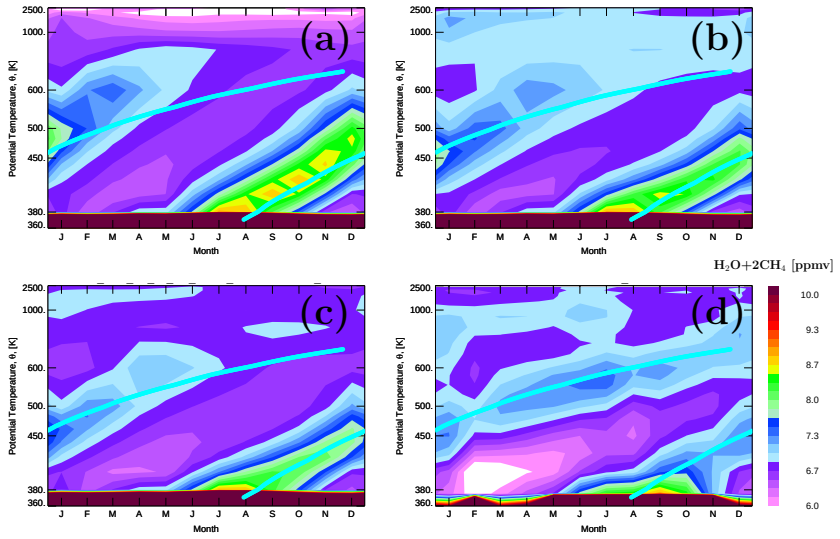

Figure 5: Representation of the tape recorder anomaly pattern ($H_2O + 2 \times CH_4$ in ppmv averaged over $\pm 10^{\circ}$N) in different CLaMS configurations (a-c) versus HALOE observations (d). In all CLaMS simulations H_2O was prescribed at $\theta \leq 380$ K by the ECMWF water vapour field and passively transported at altitude above. (a) CLaMS version described by Konopka et al. (2007, 2010) i.e. with a constant horizontal resolution (100 km) and driven by operational ECMWF analysis (with vertical velocity derived from heating rates calculated using the Morcrette radiative transfer scheme), (b) Same Lagrangian grid but ERA Interim and total diabatic heating rates (Riese et al., 2012; Ploeger et al., 2013) drive the horizontal and vertical advection, respectively, (c) Same as in (b) but with a full Lagrangian grid as described by Konopka et al. (2012), (d) HALOE climatology (Grooß and Russell, 2005) defines the cyan lines of the tape-recorder maximum (used in a-c as a reference).

The water vapour tape recorder pattern in the tropics is considered here to assess the impact of different Lagrangian grid formulations in CLaMS on the quality of the model results. The observed tape recorder pattern of the HALOE climatology (Grooß and Russell, 2005) (Fig. 5, panel d) is employed as the reference. In Fig. 5, panel (a) the simulation result is shown for the CLaMS version as described by Konopka et al. (2007, 2010); the horizontal resolution is constant

(100 km). Transport is driven by winds from the operational ECMWF analysis and vertical velocity is derived from heating rates calculated using the Morcrette radiative transfer scheme. Clearly, this model version reproduces a tape recorder pattern, albeit with a too rapid tropical upwelling. With the same Lagrangian grid, but using ERA Interim and total diabatic heating rates for driving the Lagrangian transport (Riese et al., 2012; Ploeger et al., 2013), the rate of tropical upwelling is reduced, resulting in a better agreement with observations (Fig. 5, panel b). Finally, when using the Lagrangian grid (Konopka et al., 2012, see also main body of the paper), a further improvement of the seasonality of tropical water vapour is noticeable. However, in all CLaMS versions discussed here, tropical upwelling is more rapid than observed (see also discussion in the main body of the paper).

2.3 CO and tracer patterns in the tropical region

In the main body of the paper, the anaysis focussed on anomaly patterns of CO. Here we show in addition the CO measurements by the MLS instrument averaged over the tropical regime for the time period 2005 to 2013 (Fig. 6). Further, in the main body of the paper, the tropical anomaly patterns for the long-lived tracers N_2O, CH_4, and CCl_3F (CFC-11) are shown against pressure as the vertical coordinate (Fig. 4 in the main body of the paper). Here, we show the same result, but using potential temperature as the vertical coordinate (Figs. 7 and MORE).

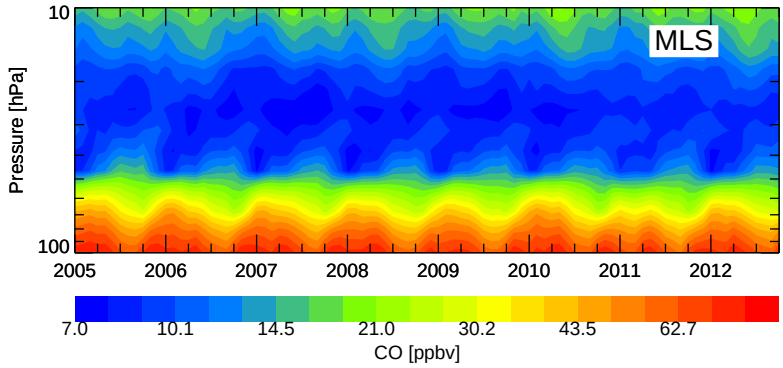

Figure 6: Measurements of CO by the MLS instrument averaged over the tropical regime ($\pm 15°$) for the time period 2005 to 2013.

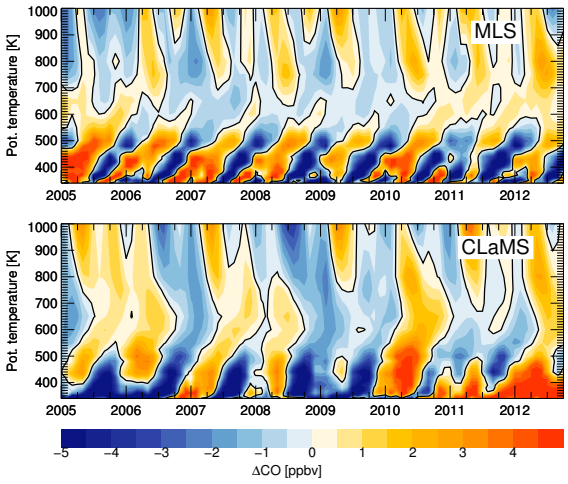

Figure 7: Comparison of CO anomalies, zonally averaged in the latitude band $\pm 15^{\circ}$ from MLS measurements (top panel) and the CLaMS simulation (bottom panel) for the time period 1 January 2005 to 31 October 2012. The CLaMS values were vertically smoothed employing the averaging kernels of the MLS measurements. The black lines in both panels indicate where the anomaly is zero. Vertical coordinate is potential temperature, in contrast to the main body of the paper where pressure was used.

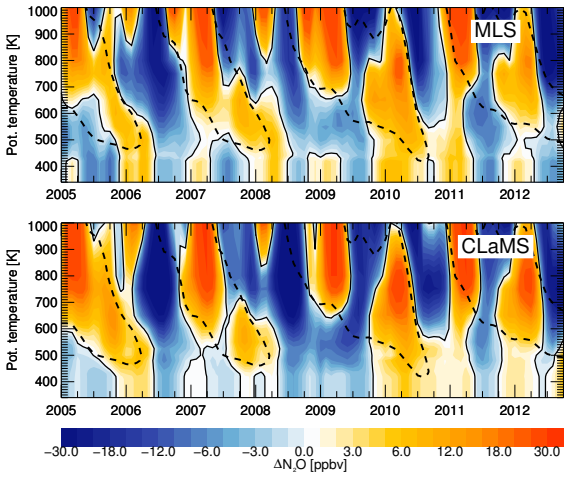

Figure 8: The anomaly pattern of tropical ($\pm 15^\circ$) N_2O as observed by MLS (top panel) and as simulated by CLaMS (bottom panel) for the time period 1 January 2005 to 31 October 2012. In contrast to Fig. 9 below, the CLaMS results are interpolated here on the MLS measurement locations and convoluted with the averaging kernels of MLS for a more accurate comparison. Dashed contours ($-15\,\mathrm{ms}^{-1}$ wind line from ERA-Interim) illustrate the easterly phase of the QBO. Vertical coordinate is potential temperature, in contrast to the main body of the paper where pressure was used.

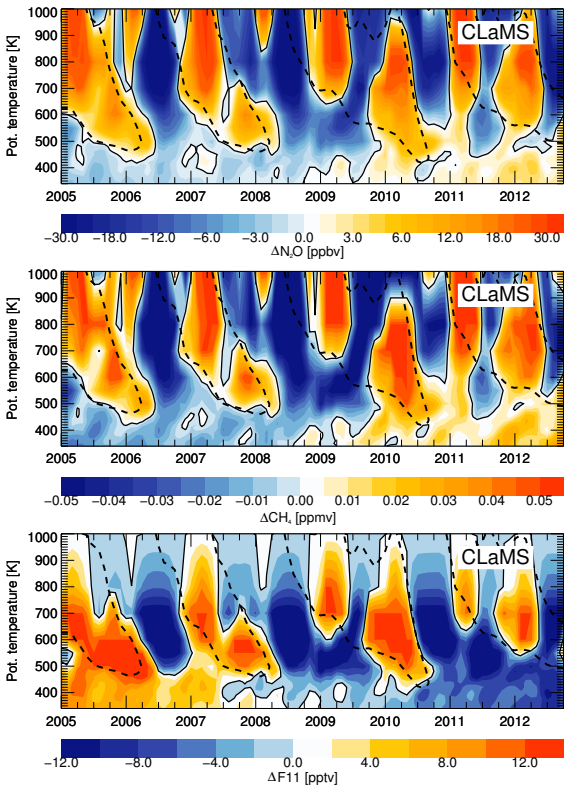

Figure 9: The anomaly pattern of tropical ($\pm 15°$) tracer fields as simulated by CLaMS for the time period 1 January 2005 to 31 October 2012. Top panel shows N_2O, middle panel CH_4, and bottom panel CCl_3F (CFC-11). Dashed contours ($-15\,\mathrm{ms}^{-1}$ wind line from ERA-Interim) illustrate the easterly phase of the QBO. Vertical coordinate is potential temperature, in contrast to the main body of the paper where pressure was used.

References

Brown, P. N., Byrne, G. D., and Hindmarsh, A. C.: VODE: A variable coefficient ODE solver, SIAM J. Sci. Stat. Comput., 10, 1038–1051, 1989.

Brunner, D., Siegmund, P., May, P. T., Chappel, L., Schiller, C., Müller, R., Peter, T., Fueglistaler, S., MacKenzie, A. R., Fix, A., Schlager, H., Allen, G., Fjaeraa, A. M., Streibel, M., and Harris, N. R. P.: The SCOUT-O3 Darwin Aircraft Campaign: rationale and meteorology, Atmos. Chem. Phys., 9, 93–117, URL `http://www.atmos-chem-phys.net/9/93/2009/`, 2009.

Cairo, F., Pommereau, J. P., Law, K. S., Schlager, H., Garnier, A., Fierli, F., Ern, M., Streibel, M., Arabas, S., Borrmann, S., Berthelier, J. J., Blom, C., Christensen, T., D'Amato, F., Di Donfrancesco, G., Deshler, T., Diedhiou, A., Durry, G., Engelsen, O., Goutail, F., Harris, N. R. P., Kerstel, E. R. T., Khaykin, S., Konopka, P., Kylling, A., Larsen, N., Lebel, T., Liu, X., MacKenzie, A. R., Nielsen, J., Oulanowski, A., Parker, D. J., Pelon, J., Polcher, J., Pyle, J. A., Ravegnani, F., Rivière, E. D., Robinson, A. D., Röckmann, T., Schiller, C., Simões, F., Stefanutti, L., Stroh, F., Some, L., Siegmund, P., Sitnikov, N., Vernier, J. P., Volk, C. M., Voigt, C., von Hobe, M., Viciani, S., and Yushkov, V.: An introduction to the SCOUT-AMMA stratospheric aircraft, balloons and sondes campaign in West Africa, August 2006: rationale and roadmap, Atmos. Chem. Phys., 10, 2237–2256, doi:10.5194/acp-10-2237-2010, 2010.

Grooß, J.-U.: Modelling of Stratospheric Chemistry based on HALOE/UARS Satellite Data, PhD thesis, University of Mainz, 1996.

Grooß, J.-U. and Russell, J. M.: Technical note: A stratospheric climatology for O_3, H_2O, CH_4, NO_x, HCl, and HF derived from HALOE measurements, Atmos. Chem. Phys., 5, 2797–2807, 2005.

Konopka, P., Günther, G., Müller, R., dos Santos, F. H. S., Schiller, C., Ravegnani, F., Ulanovsky, A., Schlager, H., Volk, C. M., Viciani, S., Pan, L. L., McKenna, D.-S., and Riese, M.: Contribution of mixing to upward transport across the tropical tropopause layer (TTL), Atmos. Chem. Phys., 7, 3285–3308, 2007.

Konopka, P., Grooß, J.-U., Günther, G., Ploeger, F., Pommrich, R., Müller, R., and Livesey, N.: Annual cycle of ozone at and above the tropical tropopause: observations versus simulations with the Chemical Lagrangian Model of the Stratosphere (CLaMS), Atmos. Chem. Phys., 10, 121–132, 2010.

Konopka, P., Ploeger, F., and Müller, R.: Entropy- and static stability-based Lagrangian model grids, in: Geophysical Monograph Series: Lagrangian Modeling of the Atmosphere, edited by Lin, J., vol. 200, pp. 99–109, American Geophysical Union, doi:10.1029/2012GM001253, 2012.

McKenna, D. S., Grooß, J.-U., Günther, G., Konopka, P., Müller, R., Carver, G., and Sasano, Y.: A new Chemical Lagrangian Model of the Stratosphere (CLaMS): 2. Formulation of chemistry scheme and initialization, J. Geophys. Res., 107, 4256, doi:10.1029/2000JD000113, 2002.

Ploeger, F., Günther, G., Konopka, P., Fueglistaler, S., Müller, R., Hoppe, C., Kunz, A., Spang, R., Grooß, J.-U., and Riese, M.: Horizontal water vapor transport in the lower stratosphere from subtropics to high latitudes during boreal summer, J. Geophys. Res., 118, 8111–8127, doi:10.1002/jgrd.50636, 2013.

Riese, M., Ploeger, F., Rap, A., Vogel, B., Konopka, P., Dameris, M., and Forster, P.: Impact of uncertainties in atmospheric mixing on simulated UTLS composition and related radiative effects, J. Geophys. Res., 117, D16305, doi:10.1029/2012JD017751, 2012.